行政院國家科學委員會專題研究計畫 成果報告

中溫固態氧化物燃料電池之關鍵零組件研發
研究成果報告(完整版)

計 畫 類 別 ：個別型
計 畫 編 號 ：NSC 96-ET-7-002-007-ET
執 行 期 間 ：96 年 01 月 01 日至 96 年 12 月 31 日
執 行 單 位 ：國立臺灣大學化學系暨研究所

計 畫 主 持 人 ：鄭淑芬

計畫參與人員：博士班研究生-兼任助理：鍾振泓、陳美如

處 理 方 式 ：本計畫可公開查詢

中 華 民 國 97 年 04 月 01 日

行政院國家科學委員會/經濟部能源局
「能源科技學術合作研究計畫」成果報告

中溫固態氧化物燃料電池之關鍵零組件研發
Research & Development of Key Components in Intermediate Temperature SOFC

計畫類別：■ 個別型計畫　　□ 整合型計畫

計畫編號：NSC96-ET-7-002-007-ET

執行期間：96 年 01 月 01 日至 96 年 12 月 31 日

計畫主持人：鄭淑芬

計畫參與人員：鍾振泓、陳美如

成果報告類型(依經費核定清單規定繳交)：□ 精簡報告
■ 完整報告

本成果報告包括以下應繳交之附件：

□赴國外出差或研習心得報告一份

□赴大陸地區出差或研習心得報告一份

□出席國際學術會議心得報告及發表之論文各一份

□國際合作研究計畫國外研究報告書一份

處理方式：除產學合作研究計畫、提升產業技術及人才培育研究計畫、列管計畫及下列情形者外，得立即公開查詢

□涉及專利或其他智慧財產權，

□一年■二年後可公開查詢

執行單位：台灣大學化學系

中　華　民　國　97　年　3　月　31　日

摘要

利用檸檬酸合成法成功製備出二氧化鈰為主體摻雜鐠之中溫固態氧化物燃料電池的電解質材料，$Ce_{1-x}Pr_xO_{2-\delta}$，x = 0.05-0.35 和鐠與鹼土金屬共摻雜之 $Ce_{0.7}Pr_{(0.3-y)}M_yO_{2-\delta}$，M = Mg 和 Ca；樣品經 1500°C 高溫燒結後，皆為單一物相之立方螢石結構。藉由 XANES 圖譜的比對，發現經 700°C 煅燒後鐠摻雜之樣品中 Pr 是以混價(3+、4+)之氧化態存在。因此，樣品中氧空缺濃度應該低於實際鐠摻雜量所應產生之氧空缺濃度。利用交流阻抗實驗測量所製備樣品的導電性，發現鐠單一摻雜之 30CPO 樣品於 700°C 具有最佳氧離子導電度 0.0668 Scm^{-1}，此數值高於目前被報導於 700℃下具有最佳氧離子導電度之 $Ce_{1-x}Gd_xO_{2-\delta}$ (0.0316 scm^{-1})與 $Ce_{1-x}Sm_xO_{2-\delta}$(0.041 Scm^{-1})電解質材料。另外，為了達到降低材料成本，嘗試引入鹼土金屬，製備雙摻雜的 CPO 材料。結果顯示，共摻雜鹼土金屬並不影響 CPO 之物相結構，以及 Ce 與 Pr 於樣品中之氧化態形式。其中，以成分組成為 $Ce_{0.7}Pr_{0.28}Mg_{0.02}O_{2-\delta}$ 是所有樣品中具有最佳導電度的材料。在還原性燃料氣氛下，添加鎂之雙摻雜的 CPMgO 材料亦顯示較佳之穩定性。

本計畫亦研究單電池之組裝，比較自燃法及非自燃法生成的 $Ce_{0.8}Gd_{0.2}O_{2-\delta}$ (CGO)粉末作為電解質，顆粒大小分別為 10 nm 及 22 nm。使用 60wt%-NiO/CGO 及 $La_{0.8}Sr_{0.2}Co_{0.8}Fe_{0.2}O_{3-\delta}$ 為陽極及陰極，以

麵粉輔助式乾壓法製備陽極負載型中溫固態氧化物燃料電池。以 5ml/min 100% H_2 為燃料及靜止空氣為氧化劑下，700℃最大功率密度及開路電壓為 250 mA/cm^2 及 0.76V；若以 100%O_2 為氧化劑，50 ml/min 100%H_2 下則可提升功率密度及開路電壓至 504 mA/cm^2 及 0.82V。

關鍵字：中溫、固態氧化物、燃料電池、二氧化鈰、組裝、單電池

Abstract

Pr-doped ceria-based electrolyte for intermediate temperature solid oxide fuel cell (IT-SOFC) was successfully synthesized by Pechini process (citric acid process). All the Pr-doped ceria (CPO) of the formula $Ce_{1-x}Pr_xO_{2-\delta}$ where x = 0.05-0.35 and those co-doped with alkaline earth of the formula $Ce_{0.7}Pr_{(0.3-y)}M_yO_{2-\delta}$, $0.01 \leqq y \leqq 0.05$ after calcination at 1500℃ were ceria based solid solution. A portion of Pr^{3+} ions doped in ceria was oxidized to Pr^{4+} during the calcination process at 700℃ in air, based on the Pr L_{III}-edge x-ray absorption near-edge spectra (XANES). As a result, lower number of oxygen vacancies was created in the samples than that expected from the original doping ratios. By using AC impedance spectroscopy, $Ce_{0.7}Pr_{0.3}O_{2-\delta}$ (30CPO) was found to give the highest conductivity of 0.0668 Scm^{-1}, which was higher than 0.0316 Scm^{-1} for $Ce_{0.8}Gd_{0.2}O_{2-\delta}$ (CGO) and 0.041 Scm^{-1} for $Ce_{1-x}Sm_xO_{2-\delta}$ (CSO), and the latter two have been reported to give the highest conductivities among ceria-based materials applied in IT-SOFC. Alkaline earths were co-doping

to CPO to reduce the cost of the materials. It was found that the crystalline phases and the oxidation states of Ce and Pr were not affected by the co-doping. Among them, $Ce_{0.7}Pr_{0.28}Mg_{0.02}O_{2-\delta}$ gave the highest conductivity. The Mg co-doping material also showed high stability in reducing environment.

We also tried to assemble single cell. Comparison was made on the CGO electrolyte powders in diameters of 10 and 22 nm prepared by citric acid method with and without auto-ignited process, respectively. The anode and cathode were 60wt%-NiO/CGO and $La_{0.8}Sr_{0.2}Co_{0.8}Fe_{0.2}O_{3-\delta}$. By using anode-supported method with the aid of flour, the resultant ITSOFC gave peak power density (PPD) and open circuit voltage (OCV) of ~250 mA/cm^2 and ~0.76V at 700℃ using 5 ml/min 100%H_2 as the fuel under static air. The PPD and OCV were raised to 504 mA/cm^2 and 0.82V using 50 ml/min 100%H_2 and 90 ml/min 100%O_2 instead of air.

Keywords：intermediate temperature, solid oxide, fuel cell, ceria, assemble, single cell

目錄

一、前言

燃料電池是一種高效、環境友好的發電裝置，它利用電化學反應直接將儲存在燃料與氧化劑中的化學能轉化為電能。固體氧化物燃料電池(SOFC)採用固體氧離子導體作為電解質，從而避免了使用液態電解質所帶來的腐蝕和電解液流失等問題，同時電池結構可靈活多樣。目前商業化之氧化物燃料電池採用 YSZ (Yttrium stabilized Zircornia) 電解質材料，其操作溫度大約需 1000°C 才具有較佳之氧離子導電率。使得在電池組裝材料選擇上需使用成本較高的耐高溫材料，以及帶來電池壽命減少的問題。相對的，二氧化鈰因其晶格氧之移動率佳，在中溫(500～700℃)範圍即有相當高之氧離子導電度。目前為止，文獻報導異元素摻雜之二氧化鈰材料以 $Ce_{1-x}Gd_xO_{2-\delta}$（CGO 或 GDC）與 $Ce_{1-x}Sm_xO_{2-\delta}$（CSO 或 SDC）具有最佳之離子導電性。但是摻雜之二氧化鈰電解質於電池實際操作條件下，會因長時間接觸陽極端所通入之燃料，導致二氧化鈰部分被還原，而有電子導電產生，進而使得氧化物燃料電池之開路電壓下降。文獻曾報導，$Ce_{0.8}Gd_{0.2}O_{1.9}$ 添加少量 Pr 可降低其於還原氣體下之電子導電率，亦有報導以固態混和法與水熱法合成 Pr-doped ceria，作為氧化物燃料電池電解質材料之研究。因 Pechini 開發之檸檬酸合成法，所得樣品分散性較為均勻，故本計畫第一部份利用此方法合成 $Ce_{1-x}Pr_xO_{2-\delta}$ 材料，並研究其離子、電子導電率

與還原氣體下導電率之穩定性。

降低 SOFC 工作溫度同時保持較高性能的關鍵是減小電池的內阻。由於傳統電解質材料的電導率隨溫度的降低而下降明顯，所以減小電解質膜的電阻至關重要。方法之一是探索具有高離子電導率的新材料。另一種方法是減小電解質膜的厚度，如將電解質負載型電池轉換成電極負載型電池。由於減小電解質膜的厚度可以降低電池的內阻，提高電池的輸出功率密度，更適合應用於 IT-SOFC。因此，在電解質的薄膜化方向，研究者相繼開發了多種薄膜製備技術，主要有電化學氣相沉積法(EVD)、化學氣相沉積法（CVD）、物理氣相沉積(PVD)、真空濺射法(Sputtering) ,等離子濺射法(Plasma spray)等物理方法，這些製備方法所需設各涉及到真空、高壓，所以機械製造複雜，成本較高。之後又發展了低成本、易操作的一些薄膜製備方法，如膠體沉積法(colloidal deposition)、刮刀成形(tape-casting),絲網印刷法(screen printing)、漿料塗覆法(slurry coating)等濕化學方法。這些濕化學方法的發明和應用推動了 IT-SOFC 的發展。由於不同材料的燒結性能及熱性能不同，以及材料間的相容性不同，目前有些電解質材料通過以上方法薄膜化後還存在一些問題，尤其是一些應用在中溫範圍內的新型電解質。

二、研究目的

本計畫第一部份利用 Pechini 方法合成 $Ce_{1-x}Pr_xO_{2-\delta}$ 材料，並研究其離子、電子導電率與還原氣體下導電率之穩定性。本計畫第二部份以低溫燃燒法生成 CGO 為基礎，建立以麵粉輔助式乾壓法製備陽極負載型 SOFC，使電解質厚度最薄下，並使氣體最佳化流速下，達到最佳的 IT-SOFC 效能。電池製程如下，陽極以含浸法製備 60wt%-NiO/CGO，電解質為 CGO，陰極以檸檬酸法合成 LSCF8282，採用自行架設的電池裝置測試效能。

三、文獻探討

燃料電池是一種高效、環境友好的發電裝置，它利用電化學反應直接將儲存在燃料與氧化劑中的化學能轉化為電能。固體氧化物燃料電池(SOFC)於採用固體氧離子導體作為電解質，從而避免了使用液態電解質所帶來的腐蝕和電解液流失等問題，同時電池結構可靈活多樣。但由於傳統的 SOFC 操作溫度過高(900～1000℃)，使得在材料選擇上使用成本較高的耐高溫材料，以及帶來電池壽命減少的問題。SOFC 原理如 Fig. 2-1 所示[1]。SOFC 採用高溫下具有傳遞氧離子能力的固體氧化物作為電解質，對氧具有還原活性的氧化物為陰極，對燃料具有催化活性的金屬或氧化物為陽極。在陰極上氧分子吸附解離後得到電

子被還原成氧離子，氧離子在電位差和氧濃度差驅動力的作用下，通過電解質中的氧空位躍遷，遷移到陽極與燃料發生氧化反應，同時釋放電子。

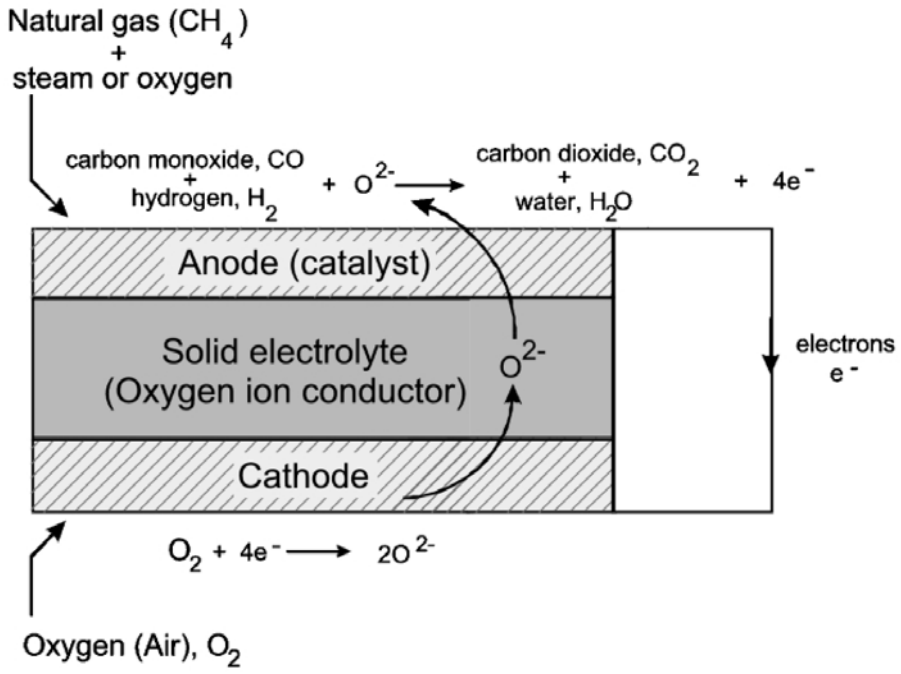

Fig. 2-1. Schematic diagram showing the general operating principles of a SOFC [1].

目前商業化之氧化物燃料電池採用 YSZ (Yttrium stabilized Zircornia) 電解質材料，其操作溫度大約需 1000°C 才具有較佳之氧離子導電率。使得在電池組裝材料選擇上需使用成本較高的耐高溫材料，以及帶來電池壽命減少的問題。相對的，中溫固體氧化物燃料電池(Intermediate Temperature SOFC，簡稱 IT-SOFC)是指在中溫(500-700℃)範圍內工作的固體氧化物燃料電池。IT-SOFC 於溫度在 800℃以下，完全可以採用成本較小的不鏽鋼材料作為雙極板，同時隨著工作溫度的降低，雖然電池的輸出性能有輕微的降低，但材料間的

化學相容性相對提高，穩定性相對增加，有利於甲烷直接氧化，最重要的是電池總成本大為降低。目前 IT-SOFC 的研究與開發主要集中在具有高氧離子電導率的新型電解質材料及電解質的薄膜化、中溫範圍內具有高催化活性的電極新材料及新材料間的相容性 [2]。

二氧化鈰因其晶格氧之移動率佳，在中溫(500～700℃)範圍即有相當高之氧離子導電度。目前為止，文獻報導異元素摻雜之二氧化鈰材料以 $Ce_{1-x}Gd_xO_{2-\delta}$（CGO 或 GDC）與 $Ce_{1-x}Sm_xO_{2-\delta}$（CSO 或 SDC）具有最佳之離子導電性。但是摻雜之二氧化鈰電解質於電池實際操作條件下，會因長時間接觸陽極端所通入之燃料，導致二氧化鈰部分被還原，而有電子導電產生，進而使得氧化物燃料電池之開路電壓下降。Maricle、Navarro 與 Lübke *et al.*曾報導過，$Ce_{0.8}Gd_{0.2}O_{1.9}$ 添加少量 Pr 可降低其於還原氣體下之電子導電率[3-5]。Balazs 與 Shuk et al.曾分別報導過以固態混和法與水熱法合成 Pr-doped ceria，作為氧化物燃料電池電解質材料之研究[6,7]。因 Pechini 開發之檸檬酸合成法，所得樣品分散性較為均勻，故本計畫第一部份利用此方法合成 $Ce_{1-x}Pr_xO_{2-\delta}$ 材料，並研究其離子、電子導電率與還原氣體下導電率之穩定性。

本計畫第二部份則研究電極負載的薄膜電解質製備技術，裝置單電池。由於減小電解質膜的厚度可以降低電池的內阻，提高電池的輸出功率密度，更適合應用於 IT-SOFC。因此，在電解質的薄膜化方向，

研究者相繼開發了多種薄膜製備技術，有電化學氣相沉積法(EVD)、化學氣相沉積法（CVD）、物理氣相沉積(PVD)、真空濺射法(Sputtering)、離子濺射法(Plasma spray)等物理方法 [8,9]。之後又發展了低成本、易操作的一些薄膜製備方法，如膠體沉積法(colloidal deposition)、刮刀成形(tape-casting)、絲網印刷法(screen printing)、漿料塗覆法(slurry coating)等濕化學方法，推動了 IT-SOFC 的發展。這些濕化學方法需要先製備出粉末樣品，固相合成法所製備粉末雖然簡單，但它難以製備出元素均勻分佈、單相、較多元素組成的粉末。而傳統濕化學方法 (如水熱合成法、共沉澱法和 sol-gel 法)所製備粉末也存在一些缺點例如，藥品成本較高，操作較複雜，時間成本較多，設備要求較多，其粉末也容易團聚和偏析。因此尋找簡單有效的快速製作粉末技術將對 SOFC 的材料研究具有特別重要的意義。本計畫以檸檬酸法配合自燃法，研製出 10 nm 粒徑的粉末，有助於製備薄膜電解。

交流阻抗在 SOFC 之電化學應用

通過交流阻抗技術觀測電化學動力學現象如 Fig. 2-2 所示[10]。交流阻抗譜圖與實軸的高頻交點代表電池的電解質電阻、電極電阻以及導線的總和（歐姆電阻），因為導線和電極界面的電阻很低一般可以忽略第一個小弧，因此近似等於電解質電阻。第二個弧為陰極/電解質界面氧離子遷移之極化電阻，而第三個弧為氧分子還原反應之極化電

阻，一般電池反應的速率控制步驟，在此三弧所代表的電化學反應比重。

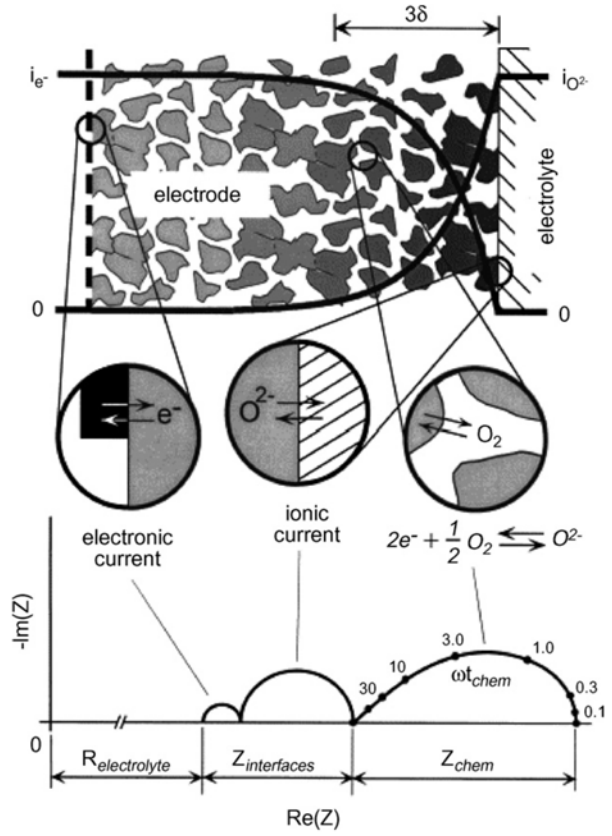

Fig. 2-2. Scheme of the cathode/electrolyte electrochemical reaction system [10].

SOFC 效能之分析

SOFC電流與電壓輸出如Fig. 2-3 [11]，因電池的功率來自輸出電位與輸出電流的貢獻（P＝IV），而實際輸出電位會隨著電池的電流密度增加而減少，這是因為電流密度增加時會使電池增加消耗歐姆過電位（IR）、活性過電位（η_{act}）及濃度過電位（η_{conc}），其基本方程式

$$V = V_{th} - IR - \eta_{act} - \eta_{conc} \quad (1)$$

，所以電池在特定輸出電位與特定輸出電流下有最大功率。

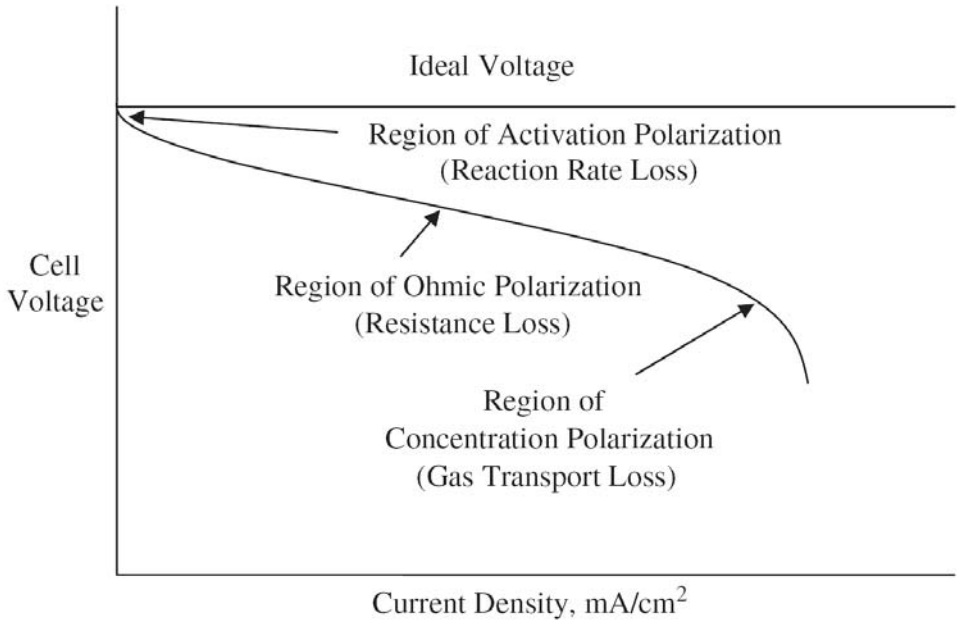

Fig. 2-3. Ideal and actual fuel cell voltage-current characteristic [11].

甘氨酸-硝酸鹽法介紹

固相合成法所製備粉末雖然最簡單，但它難以製備出元素均勻分佈、單相、較多元素組成的粉末。而傳統濕化學方法 (如水熱合成法、共沉澱法和 sol-gel 法)所製備粉末也存在一些缺點例如，藥品成本較高，操作較複雜，時間成本較多，設備要求較多，其粉末也容易團聚和偏析。因此尋找簡單有效的快速製作粉末技術將對 SOFC 的材料研究具有特別重要的意義。90 年代初，美國科學家 L.A. Chick 等[12]首先研究了甘氨酸-硝酸鹽合成法 (Glycine-nitrate process, GNP)製備出多元素氧化物，如 $La_{1-x}Sr_xCrO_{3-\delta}$、鐵電材料、超導氧化物和 NiO。主要原理：硝酸鹽金屬離子水溶液加入甘氨酸（硝酸鹽作氧化物，甘氨酸作燃料），甘氨酸當金屬離子的螯合劑使離子分散均勻外，隨水浴

溫度升高而甘氨酸（又當燃料,還原劑）被硝酸根氧化，發生自燃放熱的氧化還原反應生成金屬氧化物粉末及 H_2O, N_2, CO_2。GNP 合成法是高效節能且快速的新型合成方法，其合成溫度低，燃燒過程產生大量的氣體使粉末膨鬆，單相、多元素氧化物、比表面積大、顆粒尺寸小的超細粉體，其燃燒過程如 Fig.1-6.所示，目前該方法已廣泛被用於製備各種氧化物超細粉體。目前在 SOFC 使用上，均有使用 GNP 合成法製備陰極[13-15]、陽極[15]以及電解質粉末[15]。

四、研究方法

利用 Pechini 檸檬酸法合成鐠單一摻雜以及與鹼土金屬共摻雜之二氧化鈰材料，作為中溫氧化物燃料電池電解質層之應用。探討其於 400-700°C 下離子導電率與於 700°C 空氣與 10% H_2/N_2 氣體下之電子導電率與穩定度。Pechini 檸檬酸法合成摻雜之二氧化鈰材料，以 CGO 為例：首先蒸餾水稀釋 HNO_3 配製 10%V HNO_3 水溶液，以此作為溶劑，取 $Ce(NO_3)_3.6H_2O$ 及 $Gd(NO_3)_3.5H_2O$，配製 Ce 與 Gd 離子溶液，以體積混合得到化學計量原子莫耳組成 $Ce_{0.8}Gd_{0.2}O_{2-\delta}$，接著加入檸檬酸溶液，使 Citric acid 與總金屬離子莫耳比 1：1，並加入 PEG 以增加溶液黏度，PEG 與 Citric acid 重量比 1：60，60 ~ 70℃水浴加熱攪拌

蒸乾（濕凝膠），120℃烘箱除水（乾凝膠），研磨後接著鍛燒 700℃/4h 得到粉末（其升溫程序為室溫下 1℃/min 至 120℃恆溫 30 min，1℃/min 至 300℃恆溫 2 h，1℃/min 至目標溫度恆溫 4h），加以研磨保存。

電解質測試裝置及測試方法

將粉末研磨後取適量以不同施力 1 ton、10 ton (約 73、730M Pa) 製成約直徑 13mm 厚度 1mm 的生胚，接著高溫鍛燒 1400℃/8h 或 1500℃/14h 得到 CGO 基材（其升溫程序為，升溫速率 1℃/ min 於室溫下加熱至目標溫度 1400℃恆溫 8h、1500℃恆溫 14h）。將基材一側塗覆銀膠覆蓋銀線，接著鍛燒至 700℃/4h（其升溫程序為室溫下 1℃/ min 至 120℃恆溫 2h，1℃/ min 至 300℃恆溫 2 h，1℃/ min 至目標溫度恆溫 3h），之後將單電池另一側同樣塗覆銀膠覆蓋銀線，接著鍛燒至 750℃/4h。測量電性使用電化學交流阻抗分析儀 (EIS)，使用 Z-plot 軟體，CGO 基材為樣品，空氣中（氣體流速 50ml/min）量測不同溫度下的阻抗譜，頻率掃瞄範圍 10^6~0.01Hz，交流擾動電壓 50mV，裝置如 Fig. 4-2，測得樣品電阻 R，以厚度儀測厚，測量尺量直徑，因此根據樣品厚度 D 及面積 S 計算導電性 σ，公式為：$\sigma = D/(RS)(S.m^{-1})$。

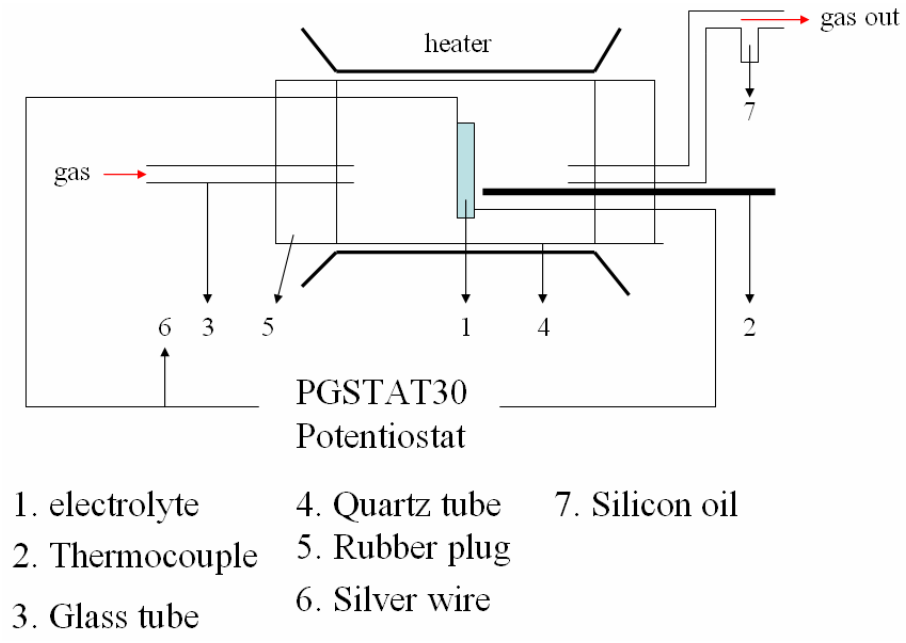

Fig. 3-1. Scheme of the electrochemical testing system.

組裝單電池時，以自燃法與非自燃法兩種途徑產生 CGO 電解質粉末，當檸檬酸法合成液在 70℃水浴加熱攪拌蒸乾成濕凝膠，置入 140℃烘箱內使自燃，將自燃後粉末經升溫程序熱處理燒掉殘餘有機物，得到粉末外觀體積大且膨鬆，稱作 fine-CGO。若將濕凝膠在 120℃烘乾除水，研磨後接著鍛燒 700℃/4h 得到粉末外觀體積小、密度高，稱作 coarse-CGO。

五、結果與討論

一、Pr 摻雜之氧化鈰電解質研究

性質鑑定

以 Pechini method 方式合成之 $Ce_{1-x}Pr_xO_{2-\delta}$ 與 $Ce_{0.7}Pr_{0.3-y}M_yO_{2-\delta}$，分別縮寫成 CPO 與 CPMO (M=Ca 與 Mg)，經由 Powder X-ray diffraction 的鑑定結果顯示，除了 35 與 40CPO 以外，其餘皆為單一螢石結構相 (Fig. 4-1)。

由於 Ce^{4+}之離子半徑(1.11Å)小於 Pr^{3+}之離子半徑(1.266Å)，因此摻雜之二氧化鈰之晶格常數隨 Pr 摻雜量增加而變大(Figure 4-2)。然而，於 CPMgO 體系下之 Mg 含量與晶格常數之關係圖顯示，晶格常數隨 Mg 含量增加而變小，因為 Mg^{2+}之離子半徑(1.03Å)小於 Pr^{3+}之離子半徑。

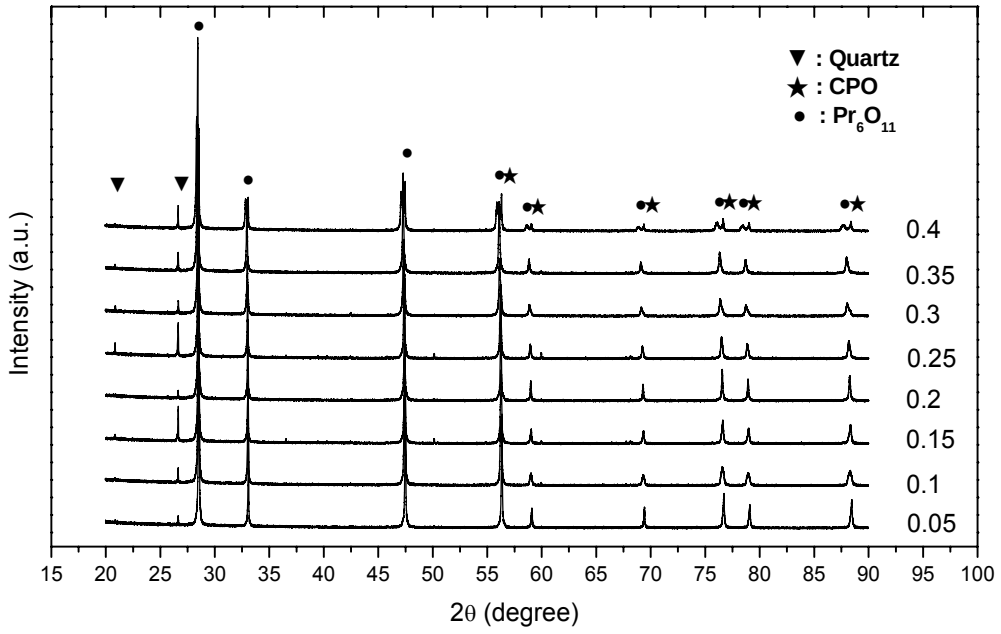

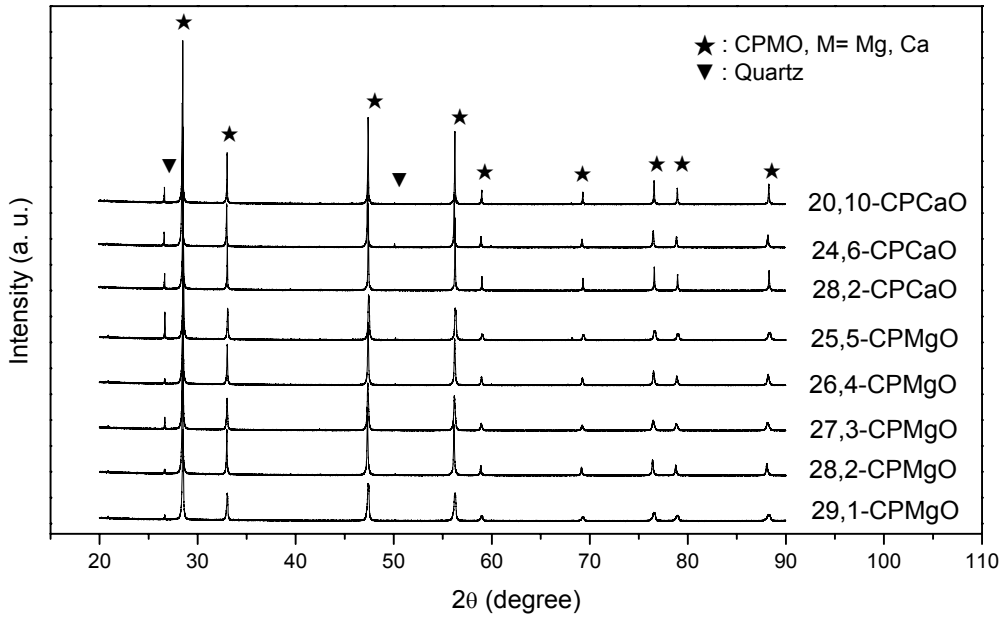

Figure 4-1. Powder XRD patterns of CPO and CPMgO, sintered at 1500°C for 14h.

Ce 與 Pr 氧化價數的鑑定採用 X-ray Absorption Near-edge Spectroscopy (XANES) technique 來作(Figure 4-3)。經由與標準品 CeO_2、Pr_2O_3 與 Pr_6O_{11} 之吸收光譜比對，結果顯示，於 CeO_2 中之 Pr 皆以 3+與 4+之氧化態存在存在。同時，測量樣品經過不同處理步驟，初合成、700°C 鍛燒與 1500°C 燒結，之 Ce 與 Pr 價數之鑑定，

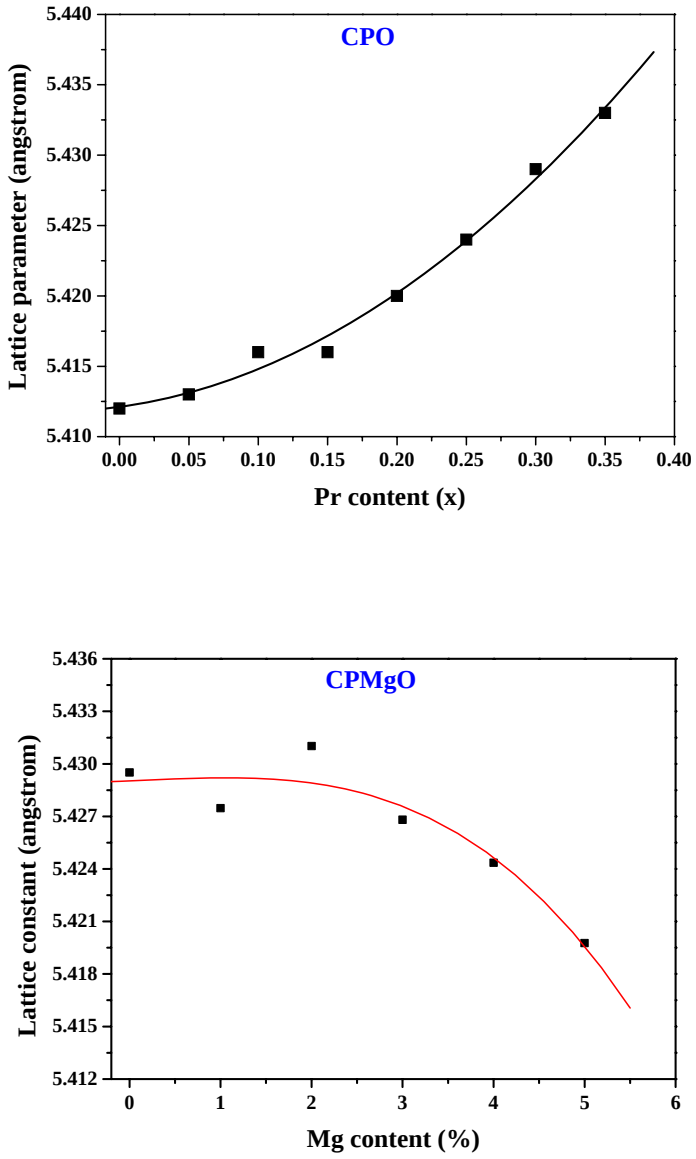

Figure 4-2. Lattice parameter as a function of x and y in $Ce_{1-x}Pr_xO_{2-\delta}$ and $Ce_{0.7}Pr_{0.3-y}Mg_yO_{2-\delta}$ sintered at 1500°C for 14h, respectively.

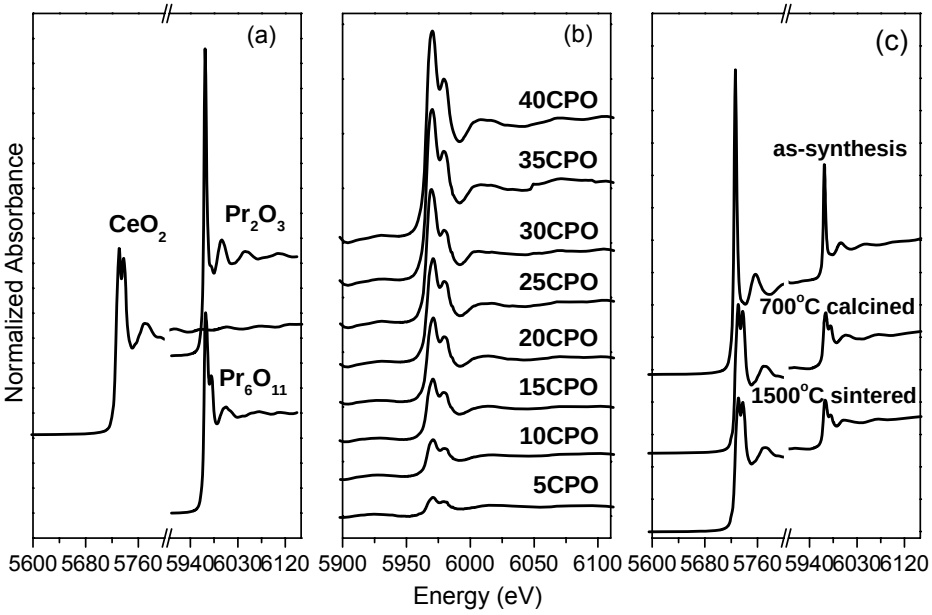

Figure 4-3. Ce and Pr L_3-edge XANES of $Ce_{1-x}Pr_xO_{2-\delta}$ after different treatments, in comparison to those of standard oxides.

實驗結果顯示，Ce^{3+}與 Pr^{3+}之起始物於 700°C 鍛燒過程中，Ce^{3+}被氧化成 Ce^{4+}，而 Pr^{3+}部分氧化 Pr^{4+}，以混價方式存在於 CeO_2 中。

離子導電性

CPO 體系之樣品於空氣 400-700°C 下的離子導電率，隨 Pr 含量與操作溫度增加而增加，如 Figure 4-4 所示。當 Ce^{4+}由 Pr^{3+}所取代時，CeO_2 必須釋出晶格氧來維持電中性。因此 CPO 材料中的氧空缺濃度隨 Pr 含量增加而增加，進而使得其氧離子導電率增加。其中，於 700°C 空氣下，以譜含量為 30% ，即 30CPO，具有最佳離子導電率，0.0668 S/cm，其高於目前文獻上所報導 $Ce_{1-x}Gd_xO_{2-\delta}$ (0.0316 S/cm) 與

$Ce_{1-x}Sm_xO_{2-\delta}$ (0.041 S/cm)之離子導電率。然而，當 Pr 含量高達 35% (x= 0.35)以上時，其材料不再維持單一螢石結構相，且其晶格變大，導致氧空缺之間的距離變大，因為 Ce^{4+} 之離子半徑（1.11Å）小於 Pr^{3+}（1.266Å）。兩者影響之下，造成 Pr 含量 35%以上，其離子導電率下降。

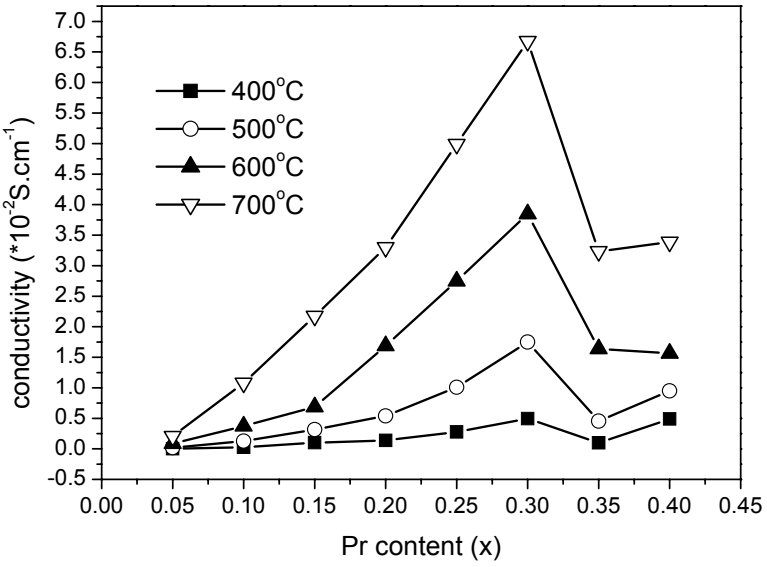

Figure 4-4. Conductivities of $Ce_{1-x}Pr_xO_{2-\delta}$, x = 0.05-0.4, as a function of x at 400-700°C in air.

為了達到降低材料成本與增加氧空缺濃度以提高離子導電率，選擇較為便宜與低氧化價數之鹼土金屬鎂與鈣來合成總摻雜量 30%之 CPMO (M=Ca and Mg)材料。研究結果發現，2% Mg 與 28%Pr 共摻雜之二氧化鈰(28,2-CPMgO)於 700°C 空氣下，具有高於 30CPO 之離子導電率，如 Figure 4-5 所示。但是，鈣的共摻雜(CPCaO)反而降低了原

先 30CPO 所表現的離子導電率。因為，Mg^{2+}的離子半徑(1.03Å)較 Pr^{3+}的氧離子半徑小(1.266Å)，因此當 Mg^{2+}取代 Pr^{3+}不僅晶格中氧空缺濃度增加，且導致晶格變小，氧空缺間的距離縮短，進而使得氧離子導電率增加。即使 Ca^{2+}之離子半徑(1.26Å)略小於 Pr^{3+}之離子半徑(1.266Å)，但是 Pr 是以 3+與 4+混合價數存在於 CeO_2 晶格中。而 Pr^{4+}之離子半徑為 1.1Å，因此 Ca^{2+}的共摻雜對於縮短氧空缺間的距離影響不大，使得導電率的提升相較於 Mg^{2+}的共摻雜是呈現負面的影響，甚至低於 25CPO 之離子導電率。

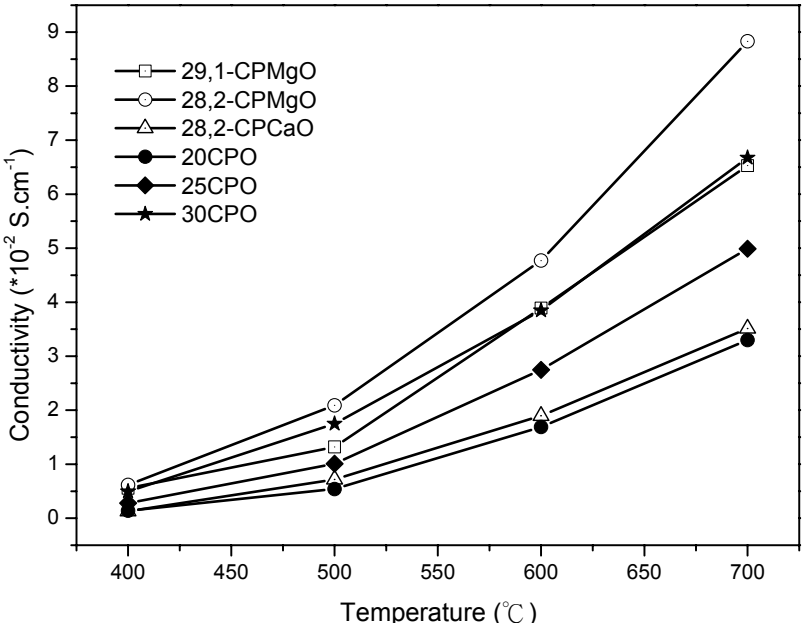

Figure 4-5. Comparison of the conductivities of CPO, CPMgO and CPCaO at 400-700°C in air.

電子導電性與穩定度

Figure 4-6 顯示 700°C 操作溫度下,操作時間對於不同氣體環境下導電率之關係圖。結果顯示，不論 CPO、CPGO 或是 CPMgO 體系，相較於同一體系，當 Pr 摻雜量增加，其 10% H_2/N_2 還原氣體下之電子導電率隨之降低。相較於 CPO、CPGO 與 CPMgO 三體系，於 CPGO 體系，隨 Gd 含量增加，其 10% H_2/N_2 氣體環境下之導電率相對減少，但是依舊高於空氣下之導電率。CPO 體系下，其 10% H_2/N_2 還原氣體下之導電率隨 Pr 含量增加而降低，其中以 25CPO 之 10% H_2/N_2 還原氣體下與空氣下之導電率相當，但是其還原氣氛下之導電率卻是隨著操作時間而衰減。然而，於 CPMgO 體系下，以 29,1-CPMgO 之還原氣體下之導電率微微低於空氣下之導電率，且隨著操作時間增加其導電率可穩定地維持。

Figure 4- . 單電池組裝

自燃法製備 CGO 電解質粉末

利用檸檬酸法製備 CGO 電解質粉末，研發出一簡單自燃法可以製備較細顆粒粉末，如 Figure 4-7 所示。700 ℃/ 4h 鍛燒後，非自燃法所得 coarse-CGO 顆粒平均粒徑 22 ± 7nm，而自燃法所得 fine-CGO 顆粒大小平均粒徑 10 ± 3nm。結果比較：非自燃法的顆粒較大，幾乎是自燃法的顆粒的二倍，因是自燃過程中瞬間高溫使得顆粒成長不及，

造成粉末密度低、體積大，並外觀上有明顯的粉末團聚現象。

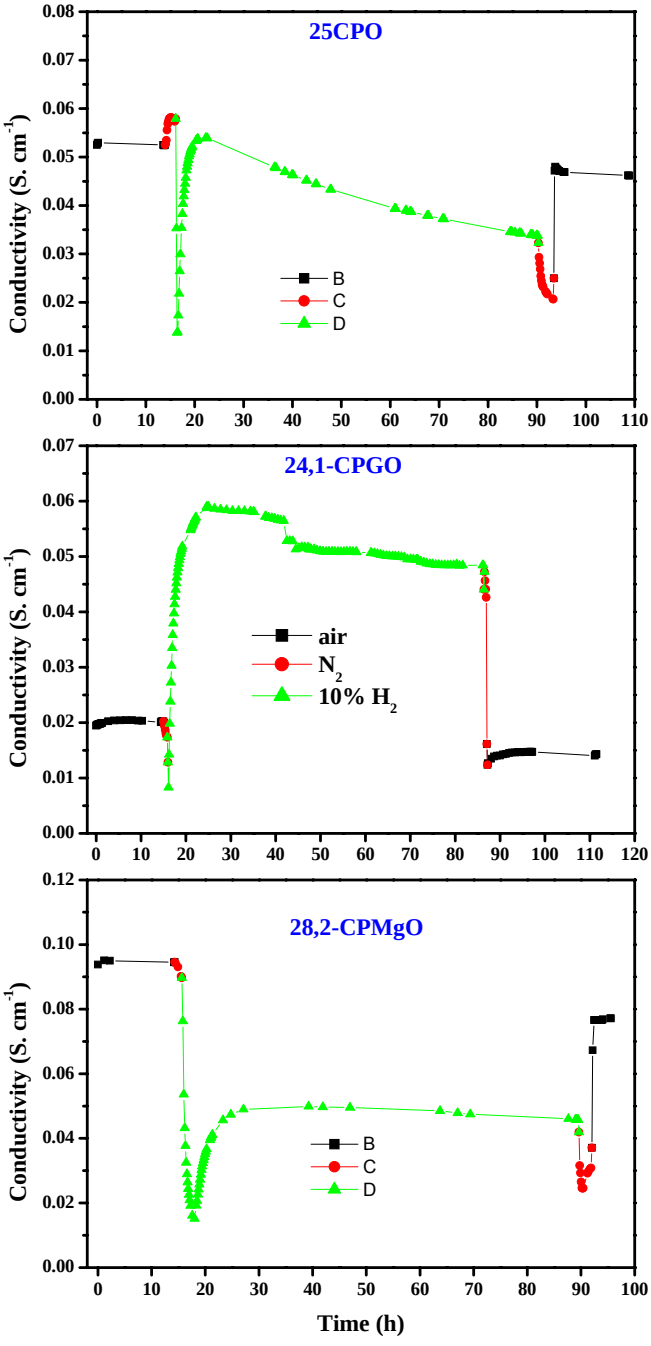

Figure 4-6. Conductivities of CPO, CPGO and CPMgO system under air, N_2 and 10% H_2/N_2 environment at 700°C.

單電池之製作及測試

取~0.3g 麵粉置入直徑 13mm 模具中，以 11 ton (～800M Pa) 加壓 10 秒，製備麵粉錠，在麵粉錠上鋪設 0.3g 陽極粉末，壓平後，在陽極粉末上鋪設適量電解質粉末，壓平後，再置入一麵粉錠至電解質粉末上端，加壓 1 ton (～73M Pa)　30 秒取出，將此樣品置於 140℃烘箱內 10 分鐘，剝離麵粉錠，得到陽極附加電解質的生胚，再於 1400℃高溫鍛燒 8h，得到陽極基材附加電解質。取適量陰極粉末 LSCF8282 加入 α-terpineol (重量比 3：5)，攪拌數分鐘再超音波震盪數分鐘，作為陰極漿料。滴陰極漿料 0.06g 於陽極基材附加電解質基材上，接著鍛燒至 1250℃/6h，即完成單電池。將單電池一側塗覆銀膠覆蓋銀線，接著鍛燒至 700℃/4h，之後將單電池另一側同樣塗覆銀膠覆蓋銀線，接著鍛燒至

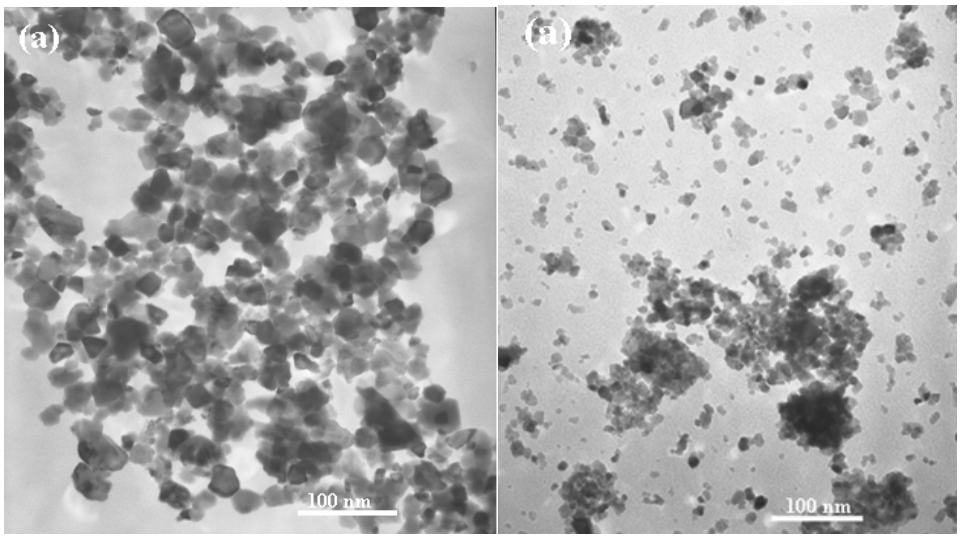

Figure 4-7. Particle sizes of CGO prepared (a) without and (b) with auto-ignition.

750℃/4h。取適量密封材料粉末加入密封膠液，將樣品之陽極側與氧化鋁管接觸，使之塗覆密封接縫處，按照商品指示乾燥，最後此接附氧化鋁管的樣品置於石英管中央，如 Figure 4-8。電極電流用銀線收集，銀線作為電極與恒電位儀連接介質，使用的是二極法連接。使用 Gpes 軟體，選擇 linear sweep voltammetry 之 normal 方式，對單電池施加電壓得到電池的反應電流，用以描述電池的輸出特性（輸出電壓及電流訊號），數據處理擷取開路電壓及最大短路電流之間範圍內 I-V 數據做功率圖譜。

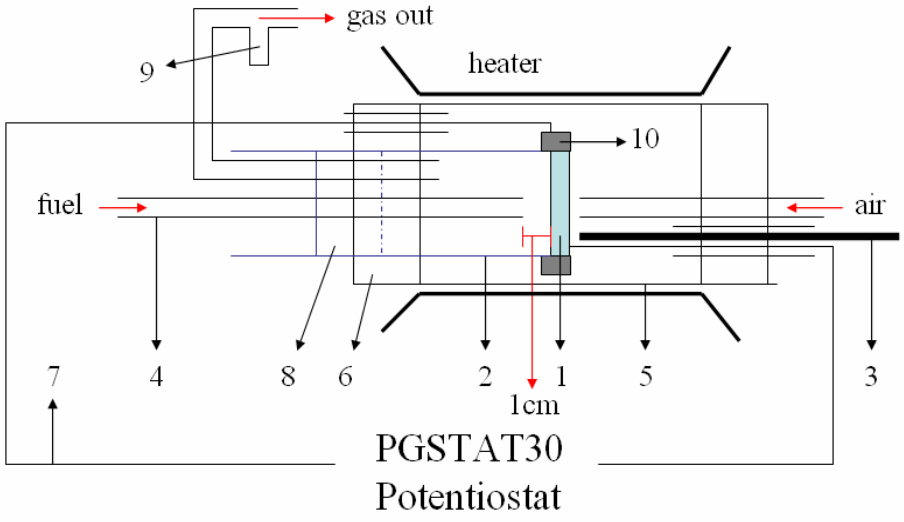

1. Single cell
2. α -Al_2O_3 tube
3. Thermocouple
4. Steel tube
5. Quartz tube
6. Quartz wool
7. Silver wire
8. Rubber plug
9. Silicon oil
10. Inorganic binder

Figure 4-8. Scheme of the electrochemical testing system.

Figure 4-9 比較自燃法所得 fine-CGO 與非自燃法所得 coarse-CGO 不

同粒徑之粉末做電解質，組裝之單電池效能。陽極以 100% H_2 為燃料，陰極為靜止空氣，電池採連續監測最大功率（PPD）及開路電壓（OCV）。以 fine-CGO 作電解質時， H_2 流速 5ml/min 下平均 PPD 為 252 mW/cm^2，若增加 H_2 流速則 PPD 會下降是因為空氣不足導致陰極極化所致；當 H_2 流速為 30ml/min 時，PPD 為 137mW/cm^2 減少約一半，若隨後回復 H_2 流速至 5ml/min 時，PPD 也可回復，表示電池製作良好 PPD 穩定性佳。此外其 OCV 隨流速趨勢與 PPD 一致，在 H_2 流速 5ml/min 下平均 OCV 為 0.76V，當流速增為 30ml/min 時，OCV 減少為 0.57V，回復 H_2 流速時，OCV 也可回復。以 coarse-CGO 作電解質時，H_2 流速 5ml/min 下平均 PPD 與 OCV 分別為 214 mW/cm^2 及 0.73V，雖然電池穩定性不差，但電池效能比 fine-CGO 做電解質時來得稍差。Figure 4-10 顯示電解質厚度從 0.04g 增加到 0.07g，其他條件不變，以 fine-CGO 做電解質時，平均 PPD 及 OCV 為 191 mW/cm^2 及 0.80V，而 coarse-CGO 做電解質時，平均 PPD 及 OCV 為 156 mW/cm^2 及 0.78V。雖然電池效率隨著電解質層厚度的增加而都有下降的現象，但 coarse-CGO 粉末所製備的電池效能仍明顯較差，因此後續研究以 fine-CGO 製備單電池，未來也將採自燃法來繼續製備電解質粉末。在增加氫氣燃料的流速至 50ml/min 與以 90ml/min 100% O_2 為氧化劑後，平均 PPD 及 OCV 可達 504 mA/cm^2 及 0.82V。

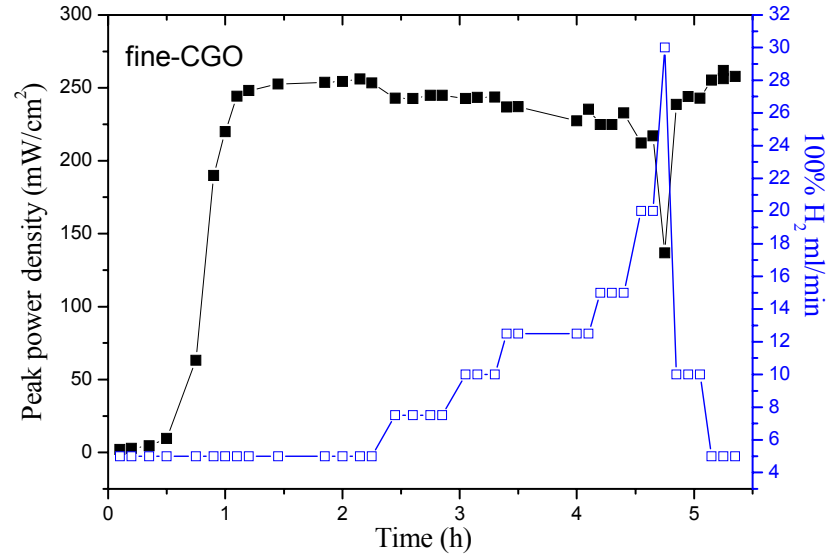
fine-CGO
Peak power density (mW/cm^2)
100% H_2 ml/min
Time (h)

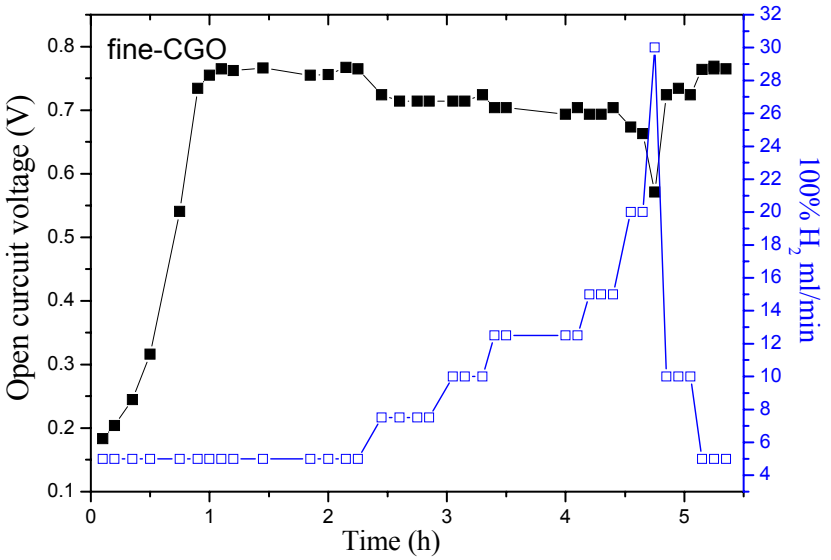
fine-CGO
Open curcuit voltage (V)
100% H_2 ml/min
Time (h)

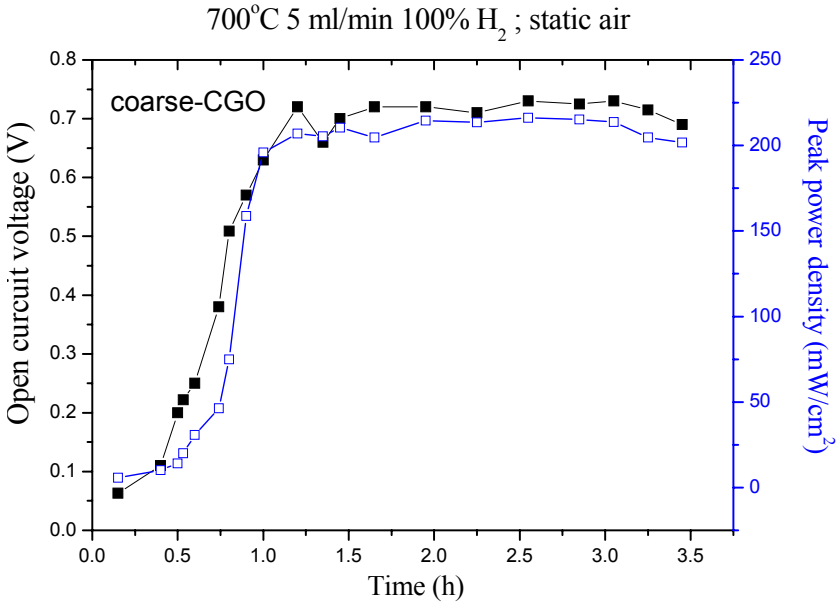

Figure 4-9. The PPD and OCV versus flow rate of 100%H_2 of single cell assembled with 0.04g CGO powders of different particle sizes.

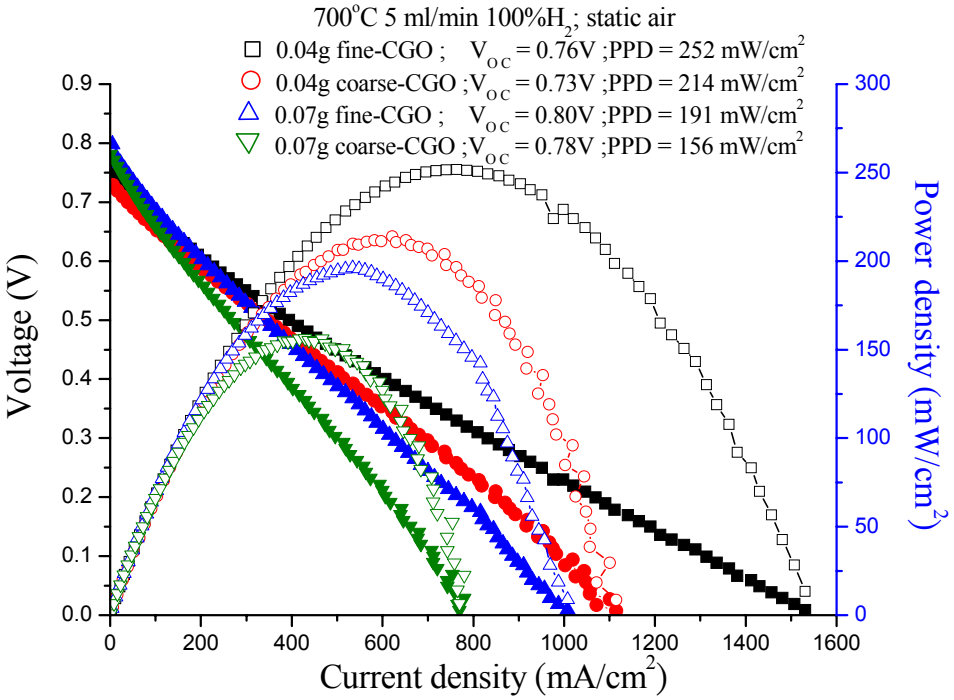

Figure 4-10. I-V and I-P curves of single cell assembled with coarse- or fine-CGO powders as electrolytes in 5ml/min 100%H_2 and static air at 700◦C.

六、計畫成果自評

以檸檬酸法可成功合成單摻雜或雙摻雜之單一螢石結構相 CeO_2。所得粉末樣品於 700°C 鍛燒後，Ce^{3+}氧化成 Ce^{4+}而 Pr^{3+}則部分氧化以混價(3+/4+)態存在於 CeO_2 晶格中。1500°C 鍛燒後之薄片中，以 30CPO 於 700°C 空氣下具有最佳離子導電率 0.0668 S/cm，高於目前文獻上報導最佳導電率之電解質材料 $Ce_{1-x}Gd_xO_{2-\delta}$ (0.0316 S/cm)與 $Ce_{1-x}Sm_xO_{2-\delta}$ (0.041 S/cm)；此部分結果已於 2007 年 6 月在日本奈良舉行之第十屆 SOFC 國際研討會發表，文章亦發表於 ETS Transactions 期刊 [16]。此外，進一步進行 Mg^{2+}的共摻雜不僅提升了原先 CPO 之離子導電率，也增進還原氣體下電子導電率之穩定性，在第二年計畫執行期間將深入探討共摻雜的影響。另一方面在組裝單電池方面，使用檸檬酸法，不需添加甘氨酸，發現在 60~70℃所得 $Ce_{0.8}Gd_{0.2}O_{2-\delta}$（CGO）濕凝膠，可於 140℃自燃得到 CGO 粉末，粉末密度低且體積大與文獻上 GNP 方法(Glycine nitrate process) 粉末特性一致，700℃鍛燒後顆粒大小約為 10 nm，稱之 fine-CGO，遠小於 120℃乾膠下 700℃鍛燒後之 22 nm 顆粒大小(稱之 coarse-CGO)。以 fine-CGO 為電解質薄膜材料，38 nm 60wt%-NiO/CGO 粉末為陽極，125 nm $La_{0.8}Sr_{0.2}Co_{0.8}Fe_{0.2}O_{3-\delta}$ (LSCF8282) 粉末為陰極，我們發展出以麵粉輔助式乾壓法組裝陽極負載型中溫固態氧化物燃料電池。50ml/min 100%H_2 作為燃料及

150ml/min 空氣作氧化劑的最佳化條件下，700℃最大功率密度及開路電壓可達 504 mA/cm^2 及 0.82V，此功率密度遠優於文獻上大部分的報導結果，而開路電壓與文獻質相近。

七、參考文獻

[1] R.M. Ormerod, Chem. Soc. Rev 32 (2003) 17.

[2] J. Molenda, K. Świerczek, W. Zając, J. Power Sources 173 (2007) 657.

[3] D.L. Maricle, T.E. Swarr, S. Karavolis, Solid State Ionics 52 (1992) 173.

[4] L. Navarro, F. Marques, J. Frade, J. Electrochem. Soc. 144 (1997) 267.

[5] S. Lübke, H.-D. Wiemhöfer, Solid State Ionics 117 (1999) 229-243

[6] G..B. Balazs, R.S. Glass, Solid State Ionics, 76 (1995) 155**.**

[7] P. Shuk, M. Greenblatt, Solid State Ionics, 116 (1999) 217**.**

[8] J. Will, A. Mitterdorfer, C. Kleinlogel, Solid State Ionics, 131 (2000) 79.

[9] G. Schiller, R. H. Henne, M. Lang, Fuel Cell Bulletin, 31 (2000) 7.

[10] Q.A. Huang, R. Hui, B. Wang , J. Zhang, Electrochimica Acta 52 (2007) 8144.

[11] K. Sadik, P. Anchasa, Y.Z. Xiang, International Journal of Hydrogen Energy 32 (2007) 761.

[12] L.A.chick, L.R. Pederson, GD. Maupin, J.L. Bates, L.E. Thomas, G.J. Exarhos, Mater. Lett. 10(1,2),(1990) 6.

[13] G. Zhu, X. Fang, C. Xia, X. Liu, Ceramics International 31 (2005) 115.

[14] B. Liu, Y. Zhang, J. Alloys Compd, doi:10.1016/j.jallcom.2006.11.142

[15] Z. Xie, W. Zhu, B. Zhu, C. Xia. Electrochimica Acta 51 (2006) 3052.

[16] M. J. Chen, F.Y. Wang, J. F. Lee, Y. L. Dai, and S. Cheng, “Study of Pr-doped Ceria-based Electrolytes for IT-SOFC”, *ECS Transactions,* 7 (2007) 2245..

八、已發表著作

ECS Transactions, 7 (1) 2245-2252 (2007)
10.1149/1.2729341, ©The Electrochemical Society

Study of Pr□doped Ceria□based Electrolytes for ITSOFC

M. J. Chen[a], S. Cheng[a] F. Y. Wang[b], J. F. Lee[c] and Y. L. Tai[c]

[a] Department of Chemistry, National Taiwan University, Taipei 106, Taiwan
[b] School of Chemistry, Huazhong Normal University, Wuhan, Hubei 430079, P. R. China
[c] National Synchrotron Radiation Research Center, Hsinchu 300, Taiwan

Pr-doped ceria materials were synthesized by Pechini method using citric acid as chelating agent, and the resultant materials were examined for possible application as electrolyte in ITSOFC. The XRD patterns of Pr doped ceria with the formula $Ce_{1-x}Pr_xO_{2-\delta}$ (abbreviated as xCPO) showed that all the samples with $x \leq 35\%$ were fluorite-type solid solutions. The Pr L_3-edge XANES profiles of xCPO after calcination at 700°C and sintering at 1500°C were similar to that of Pr_6O_{11}. For 30CPO, the $Pr^{3+}/(Pr^{3+}+Pr^{4+})$ molar ratio determined by XPS profile analysis was ca. 57%. These results implied that the number of oxygen vacancies created in the samples was lower than originally expected. Among the doped samples with x 5-40%, 30CPO gave the highest conductivity of 0.067 S/cm, which exceeded those of CGO and CSO. Moreover, with Mg co-dopant the conductivities were enhanced, while the contrary was seen with Ca co-dopant.

Introduction

Electrolyte is the key component of solid oxide fuel cells (SOFCs). Stabilized zirconia has been investigated extensively as the electrolyte material (1-7); however, stabilized zirconia electrolytes have to be operated at about 1000°C to achieve high oxide ion conductivity. At such high operating temperatures, cell performance and stability may decrease due to severe interfacial interactions or cracking between interconnector and electrolyte, electrolyte and electrodes, or electrodes and interconnector. In order to lower the operation temperature, several other solid materials have been studied and used as electrolytes, such as doped Bi_2O_3, CeO_2 and $LaGaO_3$ materials (8-14). Among them, doped ceria is considered one of the most promising as the electrolyte for intermediate temperature solid oxide fuel cells (ITSOFCs), which can be operated at 500-700°C. Among the doped ceria electrolytes, the highest conductivities were obtained on materials doped with 10-20% Gd (termed as GDC or CGO) or Sm (termed as SDC or CSO) (10-12). In addition to singly doped ceria, many studies have been carried out on co-doped samples (15-20). Among the various co-dopants, it has been shown that CGO or CSO co-doped with small amount of Pr exhibited better conductivities than singly doped ceria (15,16,22). $Ce_{0.8}Gd_{0.2-x}Pr_xO_{2-\delta}$ was found a little better than $Ce_{0.8}Gd_{0.2}O_{2-\delta}$ in both anti-reduction and ionic conductivity at 700°C (16). In 2005, Liu and coworkers also reported that a little amount of Pr co-doped with CSO could enhance ionic conductivity (22).

The singly Pr-doped ceria materials (CPO) have been reported to have applications as catalysts, as well as cathode and electrolyte materials for SOFCs (23-28). The Pr-doped

ceria materials examined as electrolytes were prepared by either conventional solid state reaction or hydrothermal method. The optimal ionic conductivity obtained by Pr-doped ceria has been close to but still lower than Gd or Sm-doped ceria (26-28). The Pechini method (29, 30), based on polymeric precursors, can be used to prepare mixed metal oxides of single phase without high temperature calcination with good stoichiometric control as well as reproducibility. The present study focuses on the preparation of Pr-doped ceria by the Pechini method and investigation of their efficiencies as electrolytes for ITSOFCs. Moreover, in order to lower the cost of raw materials and to increase the oxide vacancies, co-doping CPO with alkaline earth metals was also studied.

E□perimental

The starting materials were the nitrate salts of reagent grade (Acros) and used as purchased. The aqueous solutions of each metal ion of Ce^{3+}, Pr^{3+}, Mg^{2+} and Ca^{2+} were prepared by dissolving the nitrate salts in diluted nitrate acid and diluting them to desired concentrations. An aqueous solution of citric acid (CA) and polyethylene glycol (PEG) in a CA/PEG weight ratio of 60 was also prepared and termed as CP solution. According to the composition of the electrolyte material, different volumes of metal nitrate solutions were taken and mixed in a beaker. Then, CP solution containing citric acid of equal molar number to the total number of the metal ions in the beaker was added. The mixed solution was evaporated under stirring at 80°C until the solution became gelled. The gel was dried at 100°C, ground and calcined in air at 700°C for 4 h. The calcined sample was ground to fine powder and uniaxially pressed under 10 ton pressure into a green pellet using a stainless steel die with 13 mm diameter. The green pellet was further sintered at 1500°C for 14 h in air to form dense pellet. For structural analysis, the dense pellet was ground to powder again and a small amount of quartz powder was added as peak position reference. The X-ray diffraction (XRD) patterns were taken using a PANalytical X-ray diffractometer (Cu Kα_1, 45 kV, 40 mA). For conductivity measurement, Ag paste was brushed onto both sides of the dense pellet, and then sintered at 800°C for 30 min to form Ag electrodes. Ag wire was attached to the electrodes using Ag paste and sintered again at 800°C for 30 min. Impedance was measured using the two-probe method with a Autolab Impedance Analyzer in the frequency range of 0.01 Hz~1 MHz and with a voltage amplitude of 50 mV. The measurements were taken at constant temperatures within 400~700°C in air (50 sccm).

Results and Discussion

Characterization of Crystal Structure

The $Ce_{1-x}Pr_xO_{2-\delta}$ was abbreviated as xCPO, where x was the molar percentage of Pr^{3+} in the range of 5 to 40. All the xCPO materials with $x \leq 0.35$ sintered at 1500°C for 14h were fluorite-type solid solutions, as shown in Figure 1. When the Pr content was increased to 40%, Pr_6O_{11} phase was observed in addition to fluorite structure. Figure 2 reveals the lattice parameter of xCPO materials as a function of Pr content. The lattice expands with Pr content, due to the substitution of Ce^{4+} ions by Pr^{3+} of larger ionic radius (1.11 Å vs. 1.266 Å) (31). The variations in the crystalline structure and lattice parameter of CPO as a function of Pr content were similar to those synthesized by the hydrothermal method reported by Shuk and Greenblatt (28).

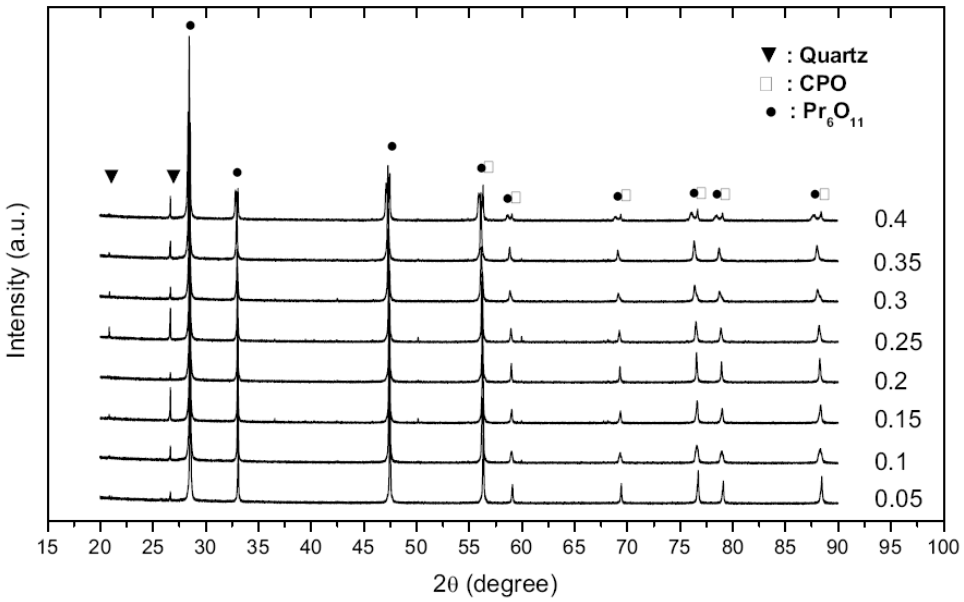

Figure 1. Powder XRD patterns of $Ce_{1-x}Pr_xO_{2-\delta}$, sintered at 1500°C for 14h, wherein x = 0.05~0.4.

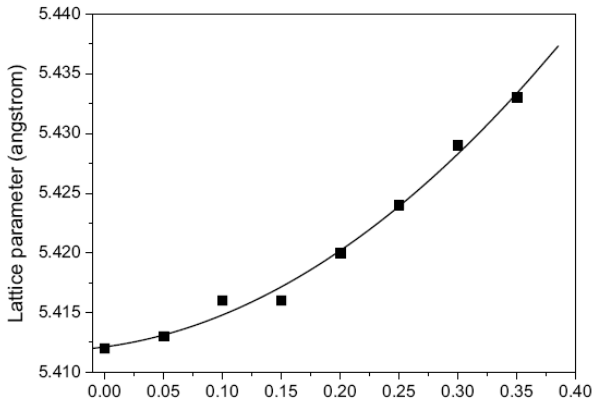

Figure 2. Lattice parameter as a function of x in $Ce_{1-x}Pr_xO_{2-\delta}$ sintered at 1500°C for 14 h.

Oxidation State of Pr

Oxidation states of Ce and Pr in CPO compounds were investigated by X-ray absorption near-edge spectroscopy (XANES) technique at beamline 17C of National Synchrotron Radiation Research Center (NSRRC), Taiwan. The Ce and Pr L_3-edge XANES spectra of CeO_2, Pr_2O_3 and Pr_6O_{11} were also taken as the references and are shown in Figure 3a. All the CPO compounds have similar XANES spectra as that of Pr_6O_{11} (Figure 3b). Both Ce and Pr in the synthesis precursors were in 3+ valence. However, a mixed valence of 3+ and 4+ was observed for Pr and only 4+ valence for Ce in the CPO compounds after they were sintered at 1500°C for 14h. In other words, all the Ce ions were oxidized from 3+ to 4+, while only a portion of the Pr ions was oxidized from 3+ to 4+. Similar phenomena were also observed by Rambabu, *et al.* (32). Since the

final electrolyte material went through three heating treatments: drying at 100°C, calcination at 700°C and sintering at 1500°C during the synthesis process, the changes in the oxidation state after these heating treatments were examined. Figure 3c shows the XANES spectra of sample 30CPO after various heating treatments. The spectrum of as-made 30CPO was similar to that of Pr_2O_3, while those after calcination and sintering were similar to that of Pr_6O_{11}. These results imply that a portion of Pr^{3+} ions doped in ceria was oxidized to Pr^{4+} during calcination at 700°C. As a result, much lower number of oxygen vacancies was created in the samples than would be expected from the original doping ratio.

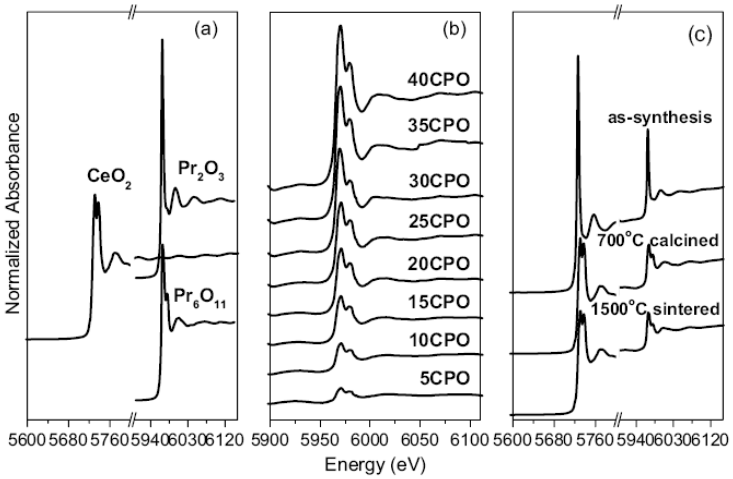

Figure 3. Ce and Pr L_3-edge XANES of $Ce_{1-x}Pr_xO_{2-\delta}$ after different treatments, in comparison to those of standard oxides.

The exact $Pr^{3+}/(Pr^{3+}+ Pr^{4+})$ ratio in the Pr-doped ceria material was determined by analyses of XPS (X-ray photoelectron spectroscopy) profiles. Figure 4 shows Pr 3d spectra of Pr_2O_3, Pr_6O_{11} and sample 30CPO after sintering at 1500°C for 14 h in air. The spectra are basically similar to those reported in the literature (33-35). The spectra of Pr_6O_{11} and 30CPO were deconvoluted using Voigt line profiles and a combined polynomial and Shirley-type background. According to the analysis by Borchert et al. (35), three spin-orbit split doublets labeled a/b, a′/b′, and a″/b″ were found in the spectrum of Pr_6O_{11}. The $3d_{3/2}$ sublevel gave an additional feature labeled ″t″, which was explained by a multiplet effect (36). Furthermore, at the high-binding-energy side, a strong oxygen Auger peak was seen. The doublet a″/b″ has been absent in the spectrum of Pr_2O_3, and therefore is assigned to Pr^{4+} ions. However, the doublets a/b and a′/b′ were present in both Pr_2O_3 and PrO_2, and they could not be assigned to either 3+ or 4+ oxidation state (36). The $Pr^{3+}/(Pr^{3+}+ Pr^{4+})$ ratio was estimated using the equation reported by Sinev *et al.* (33).

$$[Pr^{3+}]/[Pr^{3+} +Pr^{4+}]= 1- \text{area}(a'')/0.28\text{area}(a') \quad [1]$$

Accordingly, the $Pr^{3+}/(Pr^{3+}+ Pr^{4+})$ ratios for Pr_6O_{11} and 30CPO were 42.2% and 56.7%, respectively. Theoretically, the $Pr^{3+}/(Pr^{3+}+ Pr^{4+})$ ratio for Pr_6O_{11} should be 33.3%. Therefore, the ratios estimated from equation [1] are probably overestimated. Nevertheless, these results imply that about a half of the Pr ions was oxidized to 4+ after the calcination and sintering processes.

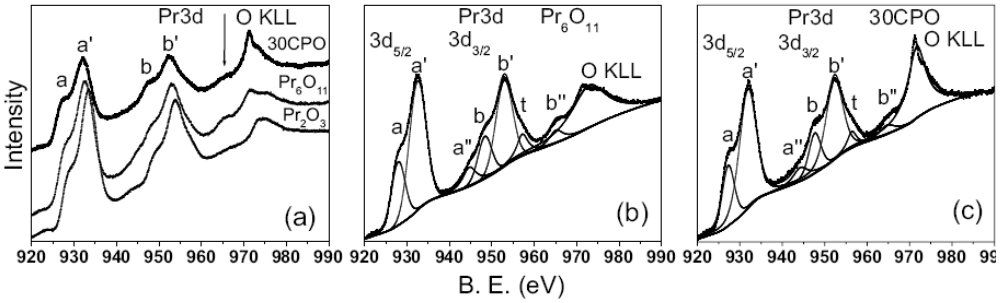

Figure 4. Pr 3d XPS spectra of (a) 30CPO after sintering at 1500°C for 14 h in air Pr_2O_3 and Pr_6O_{11}, and the deconvolution analyses of the spectra of (b) 30CPO and (c Pr_6O_{11}.

Conductivities

Figure 5 shows the conductivity (in S/cm) of xCPO measured at 400-700°C in air a function of x. It was found that the conductivity of CPO materials increased w increasing the Pr content. The maximum conductivity of 0.067 S/cm was obtained 30CPO at 700°C. This conductivity value is higher than that of CGO (Gd-doped cer and CSO (Sm-doped ceria), which are considered to give the highest conductivity amo the electrolyte materials for ITSOFC (10, 11). Similar trend in increasing conductiv with Pr content up to 30% was also observed by Shuk and Greenblatt (28), where t CPO solid solutions were synthesized by the hydrothermal method. In comparison to t conductivity ($\sigma_{700°C}$ of 0.014 S/cm) of 30CPO prepared by the hydrothermal method (2 its counterpart prepared by the Pechini method in the present study has a conductiv ($\sigma_{700°C}$ ~ 0.067 S/cm) about five times higher. However, the conductivity was found drop rapidly when the Pr content was greater than 30%. Since CPO with 35% Pr conte is still a solid solution of fluorite structure, these results are elucidated by two possil reasons: one is the decrease in movable oxide concentration as the oxygen vacan increases; the other is the increase in difficulty of oxide transportation as the latti expands with Pr content. On the other hand, the presence of an optimal Pr content in t conductivities of xCPO solid solutions also indicates that the contribution of electro conductivity to the overall conductivity in air should be negligible. The relatively hi doping Pr content (30%) to achieve maximal oxide ion conductivity of CPO, comparison to those of CGO and CSO, is attributed to that about a half of the Pr dopa is oxidized to 4+ valence. As a result, the oxygen vacancies formed in the fluorite latti should be only a half of the expected value based on the Pr content.

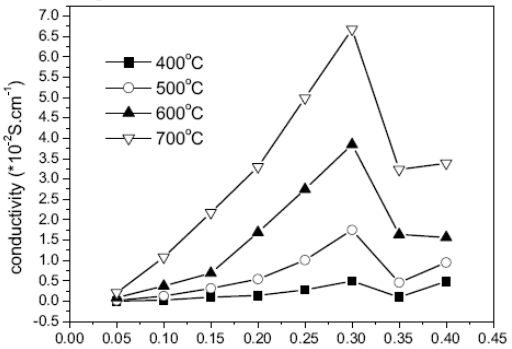

Figure 5. Conductivities of $Ce_{1-x}Pr_xO_{2-\delta}$, x = 0.05-0.4, as a function of x at 400-700°C in air.

Influence on Alkaline Earth Co-dopants

In order to reduce the cost and increase the oxygen vacancies, alkaline earth metal ions were co-doped to CPO materials. Since 30CPO gave the highest conductivity among the Pr-doped ceria. The alkaline earth co-doped CPO materials were basically replacing a small portion of Pr in 30CPO by either Mg or Ca. The materials formulated as $Ce_{0.7}Pr_{0.3-y}M_yO_{2-\delta}$. were abbreviated as x,y-CPMO, where x was the molar percentage of Pr and y is that of alkaline earth metal. The structure of CPMO materials with Mg up to 5% and Ca up to 10% were all fluorite type solid solutions, characterized by the XRD patterns shown in Figure 6. Figure 7 compares the conductivity performance of CPMO and CPO materials. Based on the equal amount of dopants, the preliminary results revealed that 28,2- and 29,1-CPMgO samples which were CPO co-doped with 2% and 1% Mg, gave higher conductivities than 30CPO, while those co-doped with Ca gave lower conductivities than 30CPO, or even lower than 25CPO. Because Mg^{2+} has lower oxidation state than Pr^{3+} or Pr^{4+}, and smaller radius (1.03Å) than that of Pr^{4+} (1.11Å), Mg^{2+} can well dissolved in the fluorite lattice and more oxygen vacancies were expected in 28,2- and 29,1-CPMgO than in 30CPO. In contrast, Ca^{2+} (1.26Å) has larger radius than Pr^{4+} (1.11Å), and co-doping Ca may result in longer distance between oxygen-oxygen vacancies. As a result, the oxide transportation is more difficult in CPCaO than in either CPMgO or CPO materials. Thus, the conductivities of CPCaO were lower than those of CPMgO and CPO.

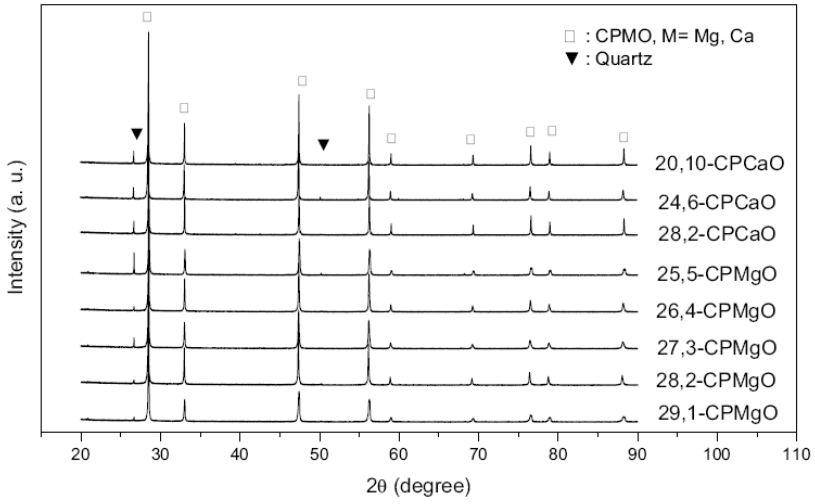

Figure 6. Powder X-ray diffraction patterns of $Ce_{0.7}Pr_{0.3-y}M_yO_{2-\delta}$, M= Mg and Ca, sintered at 1500°C for 14h in air.

Conclusions

Pr-doped ceria materials were successfully prepared by Pechini method and used as electrolytes for ITSOFC. The Ce ions in Pr-doped ceria materials were all oxidized from 3+ to 4+ during the calcination process, while only about a half of the Pr ions was oxidized based on the XPS analysis. Thus, the oxygen vacancy concentration created by Pr-dopant was only a half of the original doping value. The CPO materials doped with up

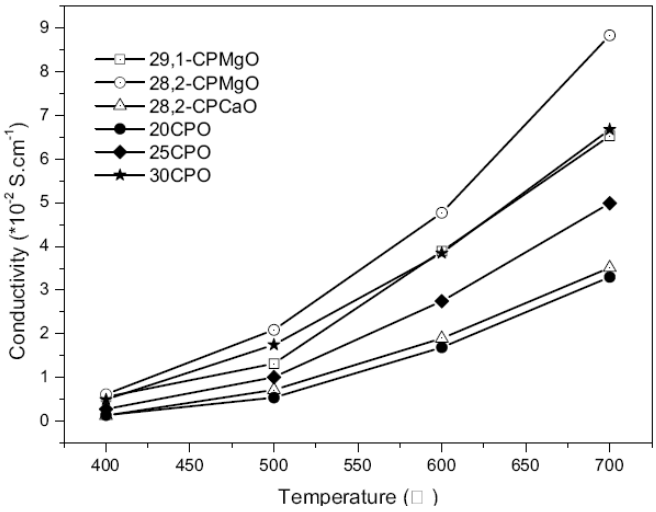

Figure 7. Comparison of the conductivities of CPO, CPMgO and CPCaO at 400-700°C in air.

to 35% Pr were solid solutions of fluorite structure. The optimal conductivity of 0.067 S.cm^{-1} was observed at 700°C in air on CPO doped with 30% Pr. That conductivity value was about five times higher than that of counterpart material prepared by the hydrothermal method (28). The presence of an optimal Pr content in the conductivities of xCPO solid solutions indicates that the contribution of electronic conductivity to the overall conductivity should be negligible. Preliminary results also revealed that the conductivity could be further enhanced by co-doping with small amount of Mg^{2+}. In contrast, co-doping with Ca^{2+} would decrease the conductivity.

Ackno□ledgments

We gratefully acknowledge the financial supports from CTCI Foundation, National Science Council and Ministry of Education, Taiwan. The assistance of Prof. Ben-Zu Wan Department of Chemical Engineering, National Taiwan University in providing AC impedance instruments is also gratefully appreciated.

References

1. T. H. Etsell, S. N. Flengas, *Chem. Rev.,* **7□**, 339, (1970).
2. B. C. H. Steele, *Sci . Ceram.,* **1□**, 1, (1980).
3. E. Subbarao, H. S. Maiti, *Solid State Ionics* **11**, 317, (1984).
4. B. C. H. Steele, *J. Power Sources* **4□**, 1, (1994).
5. V. V. Kharton, F. M. B. Marques, A. Atkinson, *Solid State Ionics,* **174**, 135, (2004).
6. S. P. S. Badwal, *Solid State Ionics*, **52**, 23, (1992).
7. S. P. S. Badwal, F. T. Ciacchi, D. Milosevic, *Solid State Ionics*, **136□137**, 91, (2000).
8. A.M. Azad, S. Larose, S.A. Akbar, *J. Mater. Sci.*, **2□**, 4135, (1994).

9. P. Shuk, H.-D. Wiemhöfer, U. Guth, W. Göpel, M. Greenblatt, *Solid State Ionics*, □, 179, (1996).
10. Z. Tianshu, P. Hing, H. Huang and J. Kilner, *Solid State Ionics* **14**□, 567, (2002).
11. R. Peng, C. Xia, Q. Fu, G. Meng and D. Peng, *Mater. Lett.,* **56**, 1043, (2002).
12. H. Inaba, H. Tagawa, *Solid State Ionics*, □**3,** 1, (1996).
13. T. Ishihara, H. Matsuda, Y. Takita, *J. Am. Chem. Soc.*, **116**, 3801, (1994).
14. J. W. Stevenson, T. R. Armstrong, L. R. Pederson, J. Li, C. A. Lewinsohn, S. Baskaran, *Solid State Ionics*, **113□115**, 571, (1998).
15. S. Lübke, H.-D. Wiemhöfer, *Solid State Ionics*, **117**, 229, (1999).
16. D. L. Maricle, T. E. Swarr, H. L. Tuller, U.S. Pat. 5,001,021, (1991)
17. J. Van Herle, D. Seneviratne, A. J. McEvoy, *J. Eur. Ceram. Soc.*, **1**□, 837, (1999)
18. T. Mori, J. Drennan, J.H. Lee, J.G. Li, T. Ikegami, *Solid State Ionics* **154□155**, 461, (2002)
19. H. Yoshida, H. Deguchi, K. Miura, M. Horiuchi, *Solid State Ionics,* **14**□, 191, (2001)
20. J. M. Ralph, J. Przydatek, J. A. Kilner, T. Seguelong, *Phys. Chem. Chem. Phys.*, **1□1**, 1403, (1997)
21. H. Yoshida, T. Inagaki, K. Miura, M. Inaba, Z. Ogumi, *Solid State Ionics*, **16**□, 109, (2003)
22. Y. Ji, J. Liu, T. He, J. Wang, W. Su, *J. Alloy. Compd.*, **3**□□, 317, (2005).
23. V. A. Sadykov, Y. V. Frolova, G. M. Alikina, A. I. Lukashevich, V. S. Muzykantov, V. A. Rogov, E. M. Moroz, D. A. Zyuzin, V. P. Ivanov, H. Borchert, E. A. Paukshtis, V. I. Bukhtiyarov, V. V. Kaichev, S. Neophytides, E. Kemnitz and K. Scheurell, *Reac. Kinet. Catal. Lett.*, □**6**, 1, (2005).
24. Y. Takasu, T. Sugino, Y. Matsuda, *J. Appl. Electrochem.*, **14**, 79, (1984).
25. M. Nauer, Ch. Fticos, B.C.H. Steele, *J. Eur. Ceram. Soc.*, **14**, 493, (1994).
26. M. Nauer, B. C. H. Steele, *J. Eur. Ceram. Soc.*, **12**, 267, (1993).
27. G. B. Balazs, R. S. Glass, *Solid State Ionics*, **76**, 155, (1995).
28. P. Shuk, M. Greenblatt, *Solid State Ionics*, **116**, 217, (1999).
29. M. P. Pechini, U.S. Pat., 3,330,697, (1967)
30. P. A. Lessing, *Amer. Soc. Ceram. Bull.*, **6**□, 1002, (1989).
31. R. D. Shannon, C. T. Prewitt, *Acta Crystallogr.*, **32A**, 751, (1976).
32. J. Hormes, M. Pantelouris, G.B. Balazs and B. Rambabu, *Solid State Ionics*, **136□137**, 945, (2000).
33. M. Yu. Sinev, G. W. Graham, L. P. Haack and M. Shelef, *J. Mater. Res.*, **11**, 1960 (1996).
34. A. Bianconi, A. Kotani, K. Okada, R. Giorgi, A. Gargano, A. Marcelli and T. Miyahara, *Phys. Rev. B*, **3**□, 3433, (1988).
35. H. Borchert, Y. V. Frolova, V. V. Kaichev, I. P. Prosvirin, G. M. Alikina, A. I. Lukashevich, V. I. Zaikovskii, E. M. Moroz, S. N. Trukhan, V. P. Ivanov, E. A. Paukshtis, V. I. Bukhtiyarov and V. A. Sadykov, *J. Phys. Chem. B*, 109, 5728, (2005).
36. H. Ogasawara, A. Kotani, R. Potze, G. A. Sawatzky and B. Thole, T. *Phys. Rev. B*, **44**, 5465, (1991).